

Order-disorder process in the tetrahedral sites of albite

ELISABETTA MENEGHINELLO,* ALBERTO ALBERTI, AND GIUSEPPE CRUCIANI

Istituto di Mineralogia, Università di Ferrara, Corso Ercole I° d'Este 32, I-44100 Ferrara, Italy

ABSTRACT

The crystal structure of albite from Stintino, Sardinia, Italy, was refined at different degrees of disorder to determine the (Si-Al) order-disorder process. Eight X-ray structure refinements were performed on single-crystal data collected at room temperature, after heating at 1050–1090 °C for 3 to 12 days. Average long-range order coefficients S between 0.93 and 0.24 were obtained for different samples. The results indicate that in the (Si-Al) disordering process Al enriches the T1m site more than T2o and T2m sites. This trend continues until both T1o and T1m are occupied by 30% of Al, and T2o and T2m by 20% of Al. No evidence of complete disorder in T1 and T2 sites has been experimentally found to date. The (Si-Al) disordering process induces a clockwise rotation of the four-membered rings of tetrahedra parallel to the (100) plane. An inverse linear relationship between the isotropic equivalent displacement parameter of the Na atom, $B_{eq}(\text{Na})$, and S is interpreted as positional disorder of Na. The variations in the Na-O bond lengths with increasing disorder are explained by the related variations in the bond strengths of tetrahedral cations.

INTRODUCTION

The unit-cell content of sodium feldspars can be represented schematically as $\text{Na}_4\text{Al}_4\text{Si}_{12}\text{O}_{32}$. The topological symmetry is monoclinic $C2/m$, whereas the real symmetry is either monoclinic $C2/m$ or triclinic $C\bar{1}$. In the monoclinic feldspars, there are only two symmetrically non-equivalent tetrahedral sites, T1 and T2, thus complete ordering is prohibited. When the symmetry is lowered to triclinic, T1 and T2 split to T1o and T1m, and to T2o and T2m, respectively, enabling complete ordering (with Al in T1o). In sodium feldspars both displacive and diffusive transformations occur, which can result in changes of symmetry. To facilitate discussion of the various possible combinations of symmetry and structural states, the following nomenclature (Griffen 1992) is used.

Monalbite is the monoclinic polymorph that can exist only at temperatures above the displacive transformation. Following Kroll and Ribbe (1983), t_i (where $t_i = \text{Al} / (\text{Al} + \text{Si})$) indicates the probability of occupying a tetrahedral T_i site with Al; thus, in monalbite $t_{1o} = t_{1m} \geq t_{2o} = t_{2m}$, with t_{1o} equal to or slightly greater than 0.25; monalbite is therefore “metrically” and “topochemically” monoclinic. Analtite is the high-temperature triclinic phase, essentially completely disordered, which inverts to monalbite on heating; analtite is “topochemically” monoclinic but “metrically” triclinic. High albite is the triclinic polymorph resulting from diffusive transformation in the (Si-Al) distribution. According to Ribbe (1983), this name should be reserved for highly disordered sodium feldspar in which the (Si-Al) distribution is “topochemically” triclinic and which cannot invert to monalbite on heating. Low albite is the low-temperature fully ordered polymorph with $t_{1o} = 1.0$ and $t_{1m} = t_{2o} = t_{2m} = 0.0$. Triclinic structural states with $t_{1o} > 0.25$ but

less than 1.0 are usually called intermediate albitites.

A long-standing problem of alkali feldspars concerns the determination of (Si-Al) order-disorder processes. These processes in alkali feldspars are usually explained by two different schemes, known as “one-step” and “two-step” paths of ordering. In the “one-step” process Al atoms migrate at the same time and at an equal rate from T1m, T2o, and T2m into T1o. The “two-step” process exhibits an initial stage with the segregation of Al in the T1 sites, followed by the ordering of Al from T1m to T1o, which causes the symmetry reduction. However, the many potassium feldspar structure refinements seem to indicate that the disordering process differs from both these schemes (Alberti and Meneghinello, in preparation).

As far as sodium feldspar is concerned, the “one-step” path of ordering is commonly accepted (Smith and Brown 1988; Ribbe 1994 and related literature), but nearly all refinements have been carried out in completely ordered low albitites or strongly disordered high albitites (only one intermediate albite is described in literature, Phillips et al. 1989). The lack of intermediate albite structure refinements does not therefore allow us to follow this order-disorder process.

To verify whether this process in sodium feldspars closely follows one of these two ideal trends, or else deviates markedly, a series of single-crystal X-ray structure refinements was performed. A natural, pure sodium feldspar was heat-treated to obtain different degrees of (Si-Al) disorder in only low albite and intermediate albitites

EXPERIMENTAL PROCEDURE

Sample description and treatment

This study of the disordering process was carried out on single crystals of albite from a green-schist meta-arenite found at Stintino, Sardinia, Italy.

The chemical analyses of Stintino albite were performed

*E-mail: mne@dns.unife.it

with an ARL-SEMQ electron microprobe operating in wave-length dispersive mode at 15 kV, with a 20 nA sample current, using a beam of 12 μm diameter. The standards used were: Amelia albite (Si, Al, Na), microcline (K), paracelsian (Ba), and synthetic An₇₀ glass (Ca); data acquisition and processing were performed by the PROBE program (Donovan 1995). Six analyses were performed on 5 different crystals; the mean chemical formula was $\text{K}_{0.004}\text{Ca}_{0.010}\text{Na}_{0.996}\text{Al}_{1.002}\text{Si}_{2.994}\text{O}_8$, with a narrow variability range around these values. $E = [\text{Al} - (\text{Na} + \text{K} + 2\text{Ca})]/(\text{Na} + \text{K} + 2\text{Ca})$ is -1.8% .

Single crystals of Stintino albite were heated in the 1050–1090 °C range for different periods between 3 and 12 days. The temperature of the furnace was measured with an accuracy of ± 5.0 °C.

In our experiments no clear relationship appeared to exist between the experimental conditions (temperature and duration of heating) and the degree of disorder reached by crystals. An obvious explanation lies in the fact that the treated samples never reached equilibrium states of order, so that factors such as crystal dimensions, presence of defects and the thermal gradient in the furnace determined the degree of disorder of the single crystals. This fact, however, did not affect our purpose, as our aim was to study the disordering process in albites rather than the equilibrium conditions for this degree of disorder.

Data collection

Single-crystal data were collected at room temperature using graphite monochromated $\text{MoK}\alpha$ radiation on a CAD-4 Enraf Nonius diffractometer in $\omega/2\theta$ scan mode, with a scan speed of 1.65° per min. The non-standard space group $C\bar{1}$ was used (with $Z = 4$) to allow comparison with literature data. Cell parameters, as refined from 25 reflections with $8^\circ < \theta < 30^\circ$, are listed in Table 1.

The SHELX76 computer program (Sheldrick 1976) was used for the structure analysis. Atomic scattering factors for neutral atoms were used. The intensity data were corrected for absorption, using the DIFABS method (Walker and Stuart

1983). $F(000)$ is 520. Refinement used a full-matrix least square fit to F with a weighing scheme of $k/\sigma^2(F)$. The number of parameters fit was 118. Refinement with anisotropic displacement factors gave a discrepancy factor wR between 3.0 and 4.5%. Corrections were made for anomalous scattering, but not extinction. Details of structure refinements for Stintino albites are reported in Table 2. After initial convergence, mean T-O bond lengths were used to estimate the Al/(Al+Si) contents for each tetrahedral site. These values were then used to adjust the scattering factors in the final stages of the refinement.

Final atomic coordinates and equivalent isotropic temperature factors are listed in Table 3. Table 4¹ contains the anisotropic displacement parameters U_{ij} (\AA^2), while Table 5¹ contains the structure factors and parameters from the last cycle of each refinement series. Finally, Table 6 reports T-O and Na-O distances (\AA).

Line-broadening analysis

The occurrence of a fine-scale cross-hatched microstructure (“tweed pattern”) in kinetically disordered materials has been predicted theoretically (Salje 1988) and observed on dark field images of albite samples annealed at 1080 °C for times exceeding 12 h but less than 144 h (Wruck et al. 1991). This was interpreted by an intra-crystalline inhomogeneity arising from local fluctuations of the degree of order within a crystal. Wruck et al. (1991) associated the development of the “tweed” structure to the line broadening of the $1\bar{3}1$ reflection as observed in synchrotron X-ray powder diffraction patterns. We collected X-ray powder patterns on the same polycrystalline material from which the crystals used for structural refinements

¹For a copy of Table 4 and Table 5, Document AM-99-015, contact the Business Office of the Mineralogical Society of America (see inside front cover of recent issue) for price information. Deposit items may also be available on the American Mineralogist web site (<http://www.minsocam.org> or current web address).

TABLE 1. Cell parameters of Stintino albites

Sample no.	<i>a</i> (\AA)	<i>b</i> (\AA)	<i>c</i> (\AA)	α ($^\circ$)	β ($^\circ$)	γ ($^\circ$)	<i>V</i> (\AA^3)
untreated	8.133(1)	12.773(5)	7.159(5)	94.23(4)	116.64(4)	87.72(2)	662.9(5)
1050-3d	8.141(2)	12.795(4)	7.145(1)	94.04(2)	116.56(2)	87.98(2)	664.1(5)
1060-6d	8.170(2)	12.811(4)	7.141(2)	93.79(3)	116.53(2)	88.09(2)	667.3(7)
1070-7d	8.140(2)	12.791(2)	7.132(1)	93.94(1)	116.54(1)	88.46(1)	662.7(2)
1080-7d	8.142(1)	12.782(2)	7.136(1)	94.00(1)	116.51(1)	88.13(1)	662.9(2)
1080-10d	8.154(2)	12.794(3)	7.129(2)	93.81(2)	116.54(2)	88.48(2)	663.9(3)
1090-7d	8.160(2)	12.802(3)	7.130(2)	93.72(2)	116.42(2)	88.61(2)	665.6(3)
1090-12d	8.152(3)	12.831(4)	7.110(2)	93.46(2)	116.52(3)	89.72(3)	663.9(4)

Note: the suffixes 3d, 6d, 7d, 10d, and 12d indicate the days of heating. Standard deviations in parentheses refer to the last digit.

TABLE 2. Details for structure refinements for Stintino albites

Samples	Temp. ($^\circ\text{C}$)	θ max. ($^\circ$)	No. unique reflections	<i>R</i>		
				$F_o > 6\sigma(F_o)$	$[F_o > 6\sigma(F_o)]$	wR $[F_o > 6\sigma(F_o)]$
Untreated	24	48	5742	3980	0.044	0.036
1050-3d	1050	40	3844	3039	0.036	0.031
1060-6d	1060	40	3678	2416	0.048	0.038
1070-7d	1070	40	3780	2804	0.044	0.034
1080-7d	1080	43	4787	4220	0.036	0.030
1080-10d	1080	42	4326	3316	0.056	0.045
1090-7d	1090	42	4660	2968	0.048	0.039
1090-12d	1090	42	4257	2970	0.060	0.044

TABLE 3. Atomic coordinates and B_{eq} for Stintino albites

	x	y	z	B_{eq} (\AA^2)	x	y	z	B_{eq} (\AA^2)
untreated					1050-3d			
T1o	0.0090(1)	0.1684(1)	0.2085(1)	0.61	0.0088(1)	0.1690(0)	0.2090(1)	0.72
T1m	0.0039(1)	0.8205(0)	0.2373(1)	0.55	0.0039(1)	0.8200(0)	0.2366(1)	0.65
T2o	0.6917(1)	0.1103(0)	0.3150(1)	0.59	0.6921(1)	0.1104(0)	0.3159(1)	0.70
T2m	0.6815(1)	0.8818(0)	0.3608(1)	0.56	0.6825(1)	0.8816(0)	0.3600(1)	0.69
OA1	0.0045(2)	0.1310(1)	0.9663(2)	0.97	0.0048(2)	0.1320(1)	0.9681(2)	1.15
OA2	0.5912(2)	0.9973(1)	0.2805(2)	0.69	0.5935(2)	0.9971(1)	0.2807(2)	0.88
OBo	0.8126(2)	0.1095(1)	0.1907(3)	1.05	0.8134(2)	0.1108(1)	0.1911(2)	1.23
OBm	0.8201(2)	0.8509(1)	0.2591(3)	1.30	0.8205(2)	0.8513(1)	0.2573(3)	1.44
OCo	0.0131(2)	0.3021(1)	0.2698(3)	0.92	0.0142(2)	0.3017(1)	0.2705(2)	1.08
OCm	0.0239(2)	0.6937(1)	0.2288(3)	0.94	0.0240(2)	0.6933(1)	0.2296(2)	1.07
ODo	0.2074(2)	0.1091(1)	0.3891(2)	0.97	0.2059(2)	0.1094(1)	0.3885(2)	1.15
ODm	0.1832(2)	0.8678(1)	0.4365(3)	1.16	0.1833(2)	0.8684(1)	0.4345(2)	1.30
Na	0.2681(1)	0.9888(1)	0.1462(2)	2.63	0.2691(1)	0.9898(1)	0.1460(2)	3.08
1060-6d					1070-7d			
T1o	0.0091(1)	0.1692(1)	0.2102(2)	0.79	0.0089(1)	0.1681(1)	0.2105(1)	0.78
T1m	0.0042(1)	0.8194(1)	0.2356(1)	0.74	0.0039(1)	0.8185(1)	0.2348(1)	0.74
T2o	0.6930(1)	0.1109(1)	0.3179(1)	0.77	0.6921(1)	0.1100(1)	0.3172(1)	0.77
T2m	0.6842(1)	0.8815(1)	0.3588(1)	0.77	0.6837(1)	0.8807(1)	0.3585(1)	0.75
OA1	0.0046(3)	0.1335(2)	0.9711(4)	1.33	0.0057(3)	0.1331(1)	0.9728(3)	1.38
OA2	0.5944(3)	0.9964(2)	0.2813(4)	1.03	0.5930(2)	0.9955(1)	0.2803(3)	1.01
OBo	0.8144(3)	0.1126(2)	0.1936(4)	1.44	0.8153(2)	0.1109(1)	0.1933(3)	1.45
OBm	0.8211(3)	0.8515(2)	0.2553(4)	1.64	0.8206(3)	0.8501(1)	0.2546(3)	1.56
OCo	0.0154(3)	0.3013(2)	0.2697(4)	1.27	0.0140(2)	0.2992(1)	0.2720(3)	1.28
OCm	0.0244(3)	0.6926(2)	0.2308(4)	1.22	0.0237(2)	0.6920(1)	0.2279(3)	1.24
ODo	0.2036(3)	0.1111(2)	0.3900(4)	1.27	0.2035(2)	0.1102(1)	0.3882(3)	1.26
ODm	0.1830(3)	0.8683(2)	0.4330(4)	1.33	0.1842(2)	0.8682(1)	0.4324(3)	1.42
Na	0.2706(2)	0.9912(1)	0.1456(3)	3.46	0.2704(2)	0.9937(1)	0.1441(2)	4.11
1080-7d					1090-12d			
T1o	0.0089(1)	0.1687(0)	0.2098(1)	0.66	0.0091(1)	0.1667(1)	0.2135(1)	0.89
T1m	0.0041(1)	0.8193(0)	0.2357(1)	0.61	0.0049(1)	0.8159(1)	0.2307(1)	0.86
T2o	0.6923(1)	0.1103(0)	0.3167(1)	0.64	0.6914(1)	0.1089(1)	0.3203(1)	0.89
T2m	0.6833(1)	0.8812(0)	0.3593(1)	0.63	0.6851(1)	0.8787(1)	0.3549(1)	0.88
OA1	0.0048(1)	0.1323(1)	0.9700(2)	1.16	0.0048(3)	0.1349(2)	0.9810(4)	1.56
OA2	0.5941(1)	0.9966(1)	0.2812(2)	0.86	0.5944(3)	0.9929(2)	0.2795(4)	1.26
OBo	0.8138(1)	0.1112(1)	0.1923(2)	1.24	0.8196(3)	0.1094(2)	0.1976(4)	1.75
OBm	0.8203(1)	0.8504(1)	0.2558(2)	1.44	0.8183(3)	0.8487(2)	0.2475(4)	1.91
OCo	0.0149(1)	0.3010(1)	0.2708(2)	1.09	0.0177(3)	0.2929(2)	0.2740(4)	1.50
OCm	0.0237(1)	0.6928(1)	0.2291(2)	1.08	0.0218(3)	0.6895(2)	0.2223(4)	1.48
ODo	0.2045(1)	0.1103(1)	0.3888(2)	1.16	0.1983(3)	0.1113(2)	0.3889(4)	1.45
ODm	0.1839(1)	0.8682(1)	0.4335(2)	1.24	0.1872(3)	0.8681(2)	0.4282(4)	1.55
Na	0.2699(1)	0.9911(1)	0.1453(1)	3.37	0.2727(2)	1.0020(2)	0.1373(3)	6.18
1080-10d					1090-7d			
T1o	0.0095(1)	0.1685(1)	0.2109(1)	0.76	0.0088(1)	0.1691(1)	0.2112(1)	0.86
T1m	0.0045(1)	0.8186(1)	0.2343(1)	0.73	0.0043(1)	0.8182(1)	0.2340(1)	0.81
T2o	0.6922(1)	0.1102(1)	0.3180(1)	0.75	0.6927(1)	0.1104(1)	0.3191(1)	0.83
T2m	0.6843(1)	0.8808(1)	0.3581(1)	0.74	0.6850(1)	0.8807(1)	0.3573(1)	0.82
OA1	0.0052(3)	0.1337(2)	0.9735(4)	1.35	0.0051(3)	0.1339(1)	0.9752(3)	1.54
OA2	0.5937(3)	0.9953(2)	0.2805(4)	1.02	0.5950(2)	0.9956(1)	0.2807(3)	1.14
OBo	0.8154(3)	0.1113(2)	0.1942(4)	1.48	0.8158(2)	0.1123(2)	0.1952(3)	1.60
OBm	0.8199(3)	0.8504(2)	0.2527(4)	1.68	0.8204(2)	0.8510(2)	0.2519(3)	1.69
OCo	0.0151(3)	0.2993(2)	0.2705(4)	1.34	0.0162(2)	0.2993(1)	0.2710(3)	1.37
OCm	0.0247(3)	0.6920(2)	0.2284(4)	1.27	0.0236(2)	0.6920(1)	0.2292(3)	1.30
ODo	0.2027(3)	0.1110(2)	0.3891(4)	1.22	0.2021(2)	0.1107(1)	0.3894(3)	1.40
ODm	0.1848(3)	0.8686(2)	0.4315(4)	1.34	0.1840(2)	0.8682(1)	0.4308(3)	1.47
Na	0.2705(2)	0.9932(2)	0.1441(3)	4.07	0.2711(2)	0.9946(1)	0.1432(2)	4.09

were extracted. In particular, sample 1050-3d was selected since its annealing time (72 h) suggested a possible occurrence of the tweed microstructure, according to Wruck et al. (1991). It is noteworthy that all other samples in this study were annealed for times exceeding 144 h. Diffraction profiles of several reflections, including the $1\bar{3}1$, were also recorded by ω -scans on single crystals used for refinements. The full width at half maximum (FWHM) of selected peaks, both from powder and single-crystal measurements, were obtained by fitting with a Pearson VII curve. As expected, we found that anisotropic line broad-

ening of powder profiles increases as a function of the degree of disorder, the increased FWHM of each peak being roughly proportional to the variation of corresponding d -spacing. The anisotropic broadening of the $1\bar{3}1$ peak is particularly striking since its d -spacing variation on disordering is one of the largest; the same extent of anisotropic broadening was not observed in the single-crystal profile data. This suggests that, for our samples, the line broadening observed in powder patterns is mostly caused by inter-crystalline inhomogeneity (i.e., internally homogeneous crystals with different degrees of disorder

TABLE 6. T-O and Na-O distances (Å) as a function of disorder

	untreated	1050-3d	1060-6d	1070-7d	1080-7d	108010d	1090-7d	1090-12d
T1o-OA1	1.748(2)	1.739(2)	1.723(2)	1.712(2)	1.727(1)	1.706(2)	1.701(2)	1.664(3)
T1o-OBo	1.742(1)	1.729(2)	1.722(2)	1.706(2)	1.721(1)	1.714(2)	1.705(2)	1.669(2)
T1o-OCo	1.729(1)	1.721(2)	1.715(2)	1.701(2)	1.714(1)	1.697(2)	1.690(2)	1.643(2)
T1o-ODo	1.740(1)	1.735(2)	1.718(2)	1.713(2)	1.722(1)	1.706(2)	1.715(2)	1.679(2)
mean	1.740	1.731	1.719	1.708	1.721	1.706	1.703	1.664
T1m-OA1	1.598(2)	1.598(2)	1.602(2)	1.614(2)	1.604(1)	1.609(2)	1.619(2)	1.636(2)
T1m-OBm	1.601(1)	1.599(2)	1.602(2)	1.599(2)	1.601(1)	1.607(2)	1.606(2)	1.630(2)
T1m-OCm	1.621(1)	1.624(1)	1.627(2)	1.622(2)	1.619(1)	1.624(2)	1.619(2)	1.627(2)
T1m-ODm	1.614(1)	1.615(2)	1.617(2)	1.620(2)	1.618(1)	1.622(2)	1.620(2)	1.632(2)
mean	1.609	1.609	1.612	1.614	1.611	1.616	1.616	1.631
T2o-OA2	1.635(1)	1.631(1)	1.646(2)	1.639(2)	1.630(1)	1.642(2)	1.637(2)	1.638(2)
T2o-OBo	1.593(1)	1.599(2)	1.601(2)	1.606(2)	1.598(1)	1.607(2)	1.608(2)	1.634(2)
T2o-OCm	1.614(2)	1.616(2)	1.614(2)	1.618(2)	1.618(1)	1.613(2)	1.623(2)	1.637(2)
T2o-ODm	1.614(2)	1.618(2)	1.615(2)	1.619(2)	1.617(1)	1.618(2)	1.619(2)	1.619(2)
mean	1.614	1.616	1.619	1.621	1.616	1.620	1.622	1.632
T2m-OA2	1.645(1)	1.645(1)	1.639(1)	1.643(1)	1.642(1)	1.639(2)	1.642(2)	1.646(2)
T2m-OBm	1.617(2)	1.618(2)	1.618(2)	1.618(2)	1.616(1)	1.618(2)	1.616(2)	1.616(2)
T2m-OCo	1.597(2)	1.598(2)	1.607(2)	1.613(2)	1.600(1)	1.612(2)	1.610(2)	1.626(2)
T2m-ODo	1.601(2)	1.608(2)	1.607(2)	1.617(2)	1.610(1)	1.614(2)	1.619(2)	1.632(2)
mean	1.615	1.617	1.618	1.623	1.617	1.621	1.622	1.630
Na-OA2	2.363(2)	2.376(2)	2.377(2)	2.358(2)	2.373(1)	2.367(2)	2.375(2)	2.357(2)
Na-ODo	2.438(2)	2.444(2)	2.480(2)	2.449(2)	2.455(1)	2.469(3)	2.472(2)	2.489(3)
Na-OBo	2.455(2)	2.468(2)	2.500(2)	2.484(2)	2.477(1)	2.491(2)	2.508(2)	2.506(2)
Na-OA1	2.529(2)	2.550(2)	2.587(2)	2.590(2)	2.564(1)	2.592(2)	2.609(2)	2.634(3)
Na-OA1	2.667(2)	2.675(2)	2.687(2)	2.657(2)	2.670(1)	2.669(3)	2.665(2)	2.660(2)
Na-OCm	3.260(2)	3.239(2)	3.217(2)	3.164(2)	3.210(1)	3.177(2)	3.151(2)	3.009(2)
Na-ODm	3.005(2)	2.995(2)	3.003(2)	3.016(2)	2.999(2)	2.999(3)	3.019(2)	3.073(4)
Na-OCo	2.965(2)	2.990(2)	3.013(2)	3.062(2)	3.014(2)	3.061(2)	3.084(2)	3.266(2)
Na-OBm	3.466(2)	3.436(2)	3.401(2)	3.383(2)	3.417(1)	3.371(2)	3.344(2)	3.242(2)

coexisting in the polycrystalline sample), instead of intra-crystalline inhomogeneity as previously reported. The absence of a strongly developed microstructure in the single crystal used is also supported by the accuracy of our structural refinement results (i.e., low wR values and low errors on coordinates comparable with those of our untreated sample, and thermal parameters physically related to the degree of disorder).

DETERMINATION OF (SI-AL) DISTRIBUTION

It is crucial to determine the aluminum content in the tetrahedral sites once the structural refinement is available. As early as 1954, Smith proposed a linear relationship between the average T-O distance of the tetrahedron and Al content of the tetrahedron itself. This relationship was subsequently implemented by Smith and Bailey (1963), Jones (1968), and Ribbe and Gibbs (1969). Ribbe (1975), Kroll and Ribbe (1983) and Ribbe (1984) devised a new linear equation, involving the individual average $\langle T-O \rangle$ distances and the “grand mean” $\langle\langle T-O \rangle\rangle$. The linear relationship of Smith (1954) was revised by Smith (1974) and by Blasi and De Pol Blasi (1994), who substituted a single straight line with a couple of straight lines with different slopes. Both Blasi and De Pol Blasi’s method (1994) and that proposed by Smith (1974) originate from the evidence that the $\langle\langle T-O \rangle\rangle$ distance is less in the disordered phases than in the ordered phases. This was interpreted by Alberti and Gottardi (1985) as indicating that, in the presence of disorder, the T-O distances (determined by structural refinement) are underestimated with respect to their true value. This means that:

$$\sum_{j=1}^n |d_j(\overrightarrow{T-O})|/n \geq \sum_{j=1}^n d_j(\overrightarrow{T-O})/n. \quad (1)$$

This difference increases as the T-O-T angle increases, hence the error varies from one tetrahedron to another. As a result, any linear relationship will underestimate the aluminum content in the disordered situations. Moreover the Si-O distances depend on numerous factors (e.g., Alberti 1996 and related literature). Hence, to calculate Al content, we use a program by Alberti and Gottardi (1988) and Alberti et al. (1990) that provides for T-O distances depending on order and other factors.

The T-O distances are calculated using

$$\text{Si-O} = 1.527 + 0.068[-\sec(\text{Si-O-Si})] \quad (2)$$

and

$$\text{Al-O} = 1.675 + 0.048[-\sec(\text{Al-O-Si})]. \quad (3)$$

In these equations, the intercepts were adjusted in such a way that the calculated mean distances $\langle\langle \text{Si-O} \rangle\rangle$ and $\langle\langle \text{Al-O} \rangle\rangle$ corresponded to the values found by the structural refinements of ordered albites (Wenk and Kroll 1984; Harlow and Brown 1980; Armbruster et al. 1990).

According to Alberti and Gottardi (unpublished data), the e.s.d. on the intercept and on the slope of regression Equation 3 was about 0.003. An analogous e.s.d. was found by Hill and Gibbs (1979) for the slope of Equation 2, but they did not report the

e.s.d. of the intercept. If we assume an e.s.d. of 0.003 for the intercept, similar to that found for the Al-O regression equation, the error propagation based on errors in the T-O distances and T-O-T angles gives an e.s.d. on t_i of about 5–6% in Al.

The aluminum content calculated in this way varies between 0.93 and 1.05; the lowest values are obtained in the phases of greatest disorder. The Al content, deduced by the linear equation of Jones (1968), varies between 0.91 and 1.07, whereas, when the method of Smith (1974) is applied, it varies between 0.85 and 0.98. The Al content obtained by Kroll and Ribbe (1983) equals 1.0 by definition. To compare the results from different methods, all these values were normalized to 1.0, and the results are reported in Table 7.

Smith and Brown (1988) defined the degree of disorder of an alkali feldspar in terms of an “average long-range order coefficient” S :

$$S = \sum_{j=1}^4 [(p_j - P_j) / (1 - P_j)] / 4 \quad (4)$$

where p_j is the fractional frequency of an atom in the j^{th} lattice node, obtained by structural refinement [i.e., Al for $j = 1$ (T1o site) and Si for $j = 2, 3, 4$ (T1m, T2o, T2m sites)], and P_j is the occupancy of the same atom in the hypothesis of a perfect disorder (i.e., in our case, $P_1 = 0.25$, and $P_2 = P_3 = P_4 = 0.75$). S therefore has values between 1.0 (complete order) and 0.0 (perfect disorder); this coefficient has the merit of expressing with a single number the degree of disorder of a phase, and is reported in Table 7.

Salje (1985) and Carpenter and Salje (1994), applying Landau's theory, introduced an “order parameter”, Q_{od} :

$$Q_{od} = (t_{1o} - t_{1m}) / (t_{1o} + t_{1m}) \quad (5)$$

where t_{1o} and t_{1m} represent the Al contents of T1o and T1m

sites. The order parameter Q_{od} also varies between 1.0 and 0.0. Q_{od} is therefore comparable with the “average long-range order coefficient” S , which will be assumed to state the degree of (Si-Al) disorder.

DISORDERING PROCESS IN ALBITE

Comparison of the data in Table 7 reveals considerable differences between the Al contents in the tetrahedral sites, depending on which method was used to calculate them. The methods of Kroll and Ribbe (1983) and Smith (1974) indicate, at high degrees of order, more order than is indicated by the method of Alberti and Gottardi (1988), or by that of Jones (1968). Jones' method, in particular, tends to show a low Al content in T1o. Methods Jones, Smith, and Kroll and Ribbe show a higher Al content in T2 sites than method Alberti and Gottardi, especially at high order, and a lower Al content in the T1m site at low order. In particular, this implies that, at the transition from monoclinic to triclinic albite, methods Jones, Smith, and Kroll and Ribbe give a sharp decrease of Al content in the T1m site: such an occurrence appears rather unlikely from a physical point of view. Hence, the remainder of the paper uses data obtained by method Alberti and Gottardi.

In the most ordered phase (low albite), aluminum is almost entirely concentrated in T1o, and only small percentages of Al are more or less equally distributed in the other three sites. When the disordering process begins, we can follow the migration of aluminum from T1o to the other sites (T1m, T2o, and T2m). It is evident that Al enriches T1m more than it does T2o and T2m, and that this difference increases proportionally with the increase of the aluminum migration from T1o. The intermediate state of disordering is reached in the so-called intermediate albite (see also Phillips et al. 1989). In this phase about 45% Al is concentrated in T1o, whereas about 25% Al is found in T1m, and about 16% Al in T2o and T2m. The triclinic symmetry of

TABLE 7. Al-content [Al/(Al+Si)] in tetrahedral sites of albites

	A&G t1o	A&G t1m	A&G t2o	A&G t2m	J t1o	J t1m	J t2o	J t2m	Sm t1o	Sm t1m	Sm t2o	Sm t2m	K&R t1o	K&R t1m	K&R t2o	K&R t2m	S
Low Albite*	0.93	0.04	0.01	0.02	0.81	0.04	0.07	0.08	0.97	-0.02	0.02	0.03	0.98	-0.02	0.01	0.03	0.91
Low Albite†	0.95	0.02	0.01	0.02	0.83	0.02	0.07	0.08	0.98	-0.04	0.02	0.03	1.00	-0.04	0.02	0.02	0.93
Low Albite‡	0.93	0.04	0.01	0.02	0.81	0.04	0.07	0.08	0.97	-0.02	0.02	0.03	0.98	-0.02	0.01	0.03	0.91
Untreated	0.96	0.03	0.00	0.01	0.83	0.04	0.06	0.07	0.99	-0.02	0.01	0.02	0.98	-0.01	0.01	0.02	0.93
1050-3d	0.91	0.04	0.02	0.03	0.80	0.03	0.08	0.09	0.95	-0.02	0.03	0.04	0.92	-0.01	0.04	0.05	0.88
1060-6d	0.84	0.07	0.05	0.04	0.75	0.06	0.10	0.09	0.89	0.00	0.06	0.05	0.85	0.02	0.07	0.06	0.79
1070-7d	0.78	0.08	0.06	0.08	0.69	0.07	0.11	0.13	0.82	0.01	0.08	0.09	0.76	0.04	0.09	0.11	0.71
1080-7d	0.90	0.05	0.02	0.03	0.78	0.05	0.08	0.09	0.93	-0.01	0.03	0.04	0.86	0.02	0.06	0.06	0.87
1080-10d	0.78	0.10	0.06	0.06	0.69	0.08	0.11	0.12	0.82	0.03	0.07	0.08	0.75	0.06	0.09	0.10	0.71
1090-7d	0.75	0.10	0.08	0.07	0.67	0.09	0.12	0.12	0.78	0.04	0.09	0.09	0.73	0.06	0.11	0.10	0.66
1090-12d	0.43	0.25	0.17	0.15	0.42	0.19	0.20	0.19	0.47	0.18	0.19	0.16	0.44	0.19	0.19	0.18	0.24
Int. Albite§	0.46	0.23	0.15	0.16	0.46	0.17	0.18	0.19	0.51	0.15	0.16	0.17	0.51	0.15	0.16	0.17	0.28
High Albite	0.26	0.30	0.22	0.22	0.27	0.24	0.24	0.25	0.28	0.24	0.24	0.24	0.28	0.24	0.24	0.24	0.08
High Albite#	0.27	0.30	0.21	0.22	0.29	0.24	0.23	0.24	0.30	0.24	0.23	0.24	0.30	0.24	0.22	0.24	0.09
Monalbite#	0.30		0.20		0.28		0.22		0.29		0.21		0.29		0.21		

Notes: A&G: Alberti and Gottardi (1988); J: Jones (1968); Sm: Smith (1974); K&R: Kroll and Ribbe (1983).

S: average long-range order coefficient (Smith and Brown, 1988); Al content from A&G method was used to calculate S. The esd on t_i is 5–6% of Al using the A&G method.

* Wenk and Kroll (1984).

† Harlow and Brown (1980).

‡ Armbruster et al. (1990).

§ Phillips et al. (1989).

|| Prewitt et al. (1976).

#Winter et al. (1979).

albite is maintained as long as up to about 30% Al is present in T1o and T1m, and about 20% Al in T2o and T2m (high albite). Monalbite also (Winter et al. 1979) shows 30% Al in the T1 site and 20% Al in the T2 site, and that no experimental evidence exists of complete disorder in sodium feldspar. From Figure 1 the T1m tetrahedron follows a different trend with respect to T2o and T2m: in fact, Al enriches the T1m site more than the T2 sites.

Kunz and Armbruster (1990) showed that difference values $\langle\Delta U\rangle$ along the (Si-Al)-O vector in alkali feldspar tetrahedra, calculated by anisotropic mean-square displacement parameters, provide information on static and dynamic (Si-Al) disorder. They thus derived a theoretical model that correlates $\langle T-O\rangle$ and $\langle\Delta U\rangle$, and showed that theoretically predicted $\langle\Delta U\rangle$ values are in good agreement with those observed. The close correspondence between our data and those reported by Kunz and Armbruster (1990) is evident in Figure 2, confirming the dependence of $\langle\Delta U\rangle$ on the degree of (Si-Al) disorder, as well as the presence of static disorder of oxygen atoms when (Si-Al) substitution occurs in alkali feldspars.

These variations of the x atomic coordinate with degree of disorder tend to be small (Fig. 3²), but the other two are markedly greater, often reaching high levels (as much as 50–60 σ). The shifts of tetrahedral atoms indicate that a clockwise rotation of the four-membered tetrahedral rings, in a manner essentially parallel to the (100) plane as depicted in Figure 4, occurs during the disordering process.

Disorder leads to a normalization of the bond strength on O atoms (Table 8). The standard deviation Δ on anions, which for low temperature albite is 0.073, descends gradually to as little as 0.027 in the strongly disordered phases. Hence, OCo moves away from sodium in the order-disorder transformation, due to

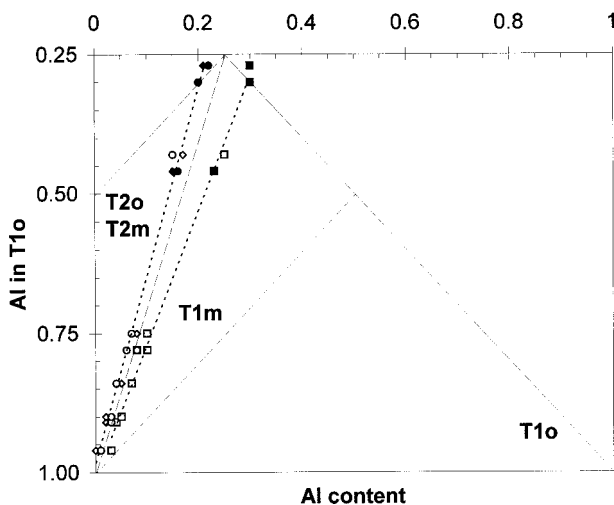


FIGURE 1. Disordering process in sodium feldspars. Solid lines represent the ideal “two-step” path, while the long dashed line represents the “one-step.” Dotted lines report the disorder trend derived from our method. Empty symbols indicate our albites, while filled symbols represent samples taken from literature (squares = T1m, diamonds = T2o, and circles = T2m).

the increase of the tetrahedral charge on OCo itself from 1.75 to 1.875, whereas OBm and OCm approach Na, as the charge acting on these O atoms varies from 2.0 to 1.875. Similar patterns are also found for the other O atoms, although the variations in Na-O distances are less pronounced.

EFFECTS OF DISORDER ON THE SODIUM ATOM

$B_{eq}(\text{Na})$ as a function of disorder

The isotropic thermal parameters, $B_{eq}(\text{Na})$ (Table 3), increase as the degree of disorder rises. Because all the data collections were performed at room temperature, such an increase must be attributed to positional disorder connected with (Si-Al) substitution in the tetrahedral sites, which is in turn also reflected in a positional disorder of the framework O atoms (Alberti and

TABLE 8. Bond strength on O atoms for different S values

	untreated (S = 0.93)	1070-7d (S = 0.71)	1090-12d (S = 0.24)	High Albite* (S = 0.08)
OA1	2.00	2.02	2.07	2.08
OA2	2.08	2.07	2.04	2.02
OBo	1.92	1.94	1.98	2.01
OBm	2.07	2.06	1.99	1.99
OCo	1.88	1.89	1.96	1.96
OCm	2.06	2.04	1.99	1.97
ODo	1.91	1.93	1.97	2.00
ODm	2.08	2.05	2.00	1.97
Δ	0.073	0.052	0.027	0.027

Notes: Calculated according to Ferguson (1974).

* Prewitt et al. 1976.

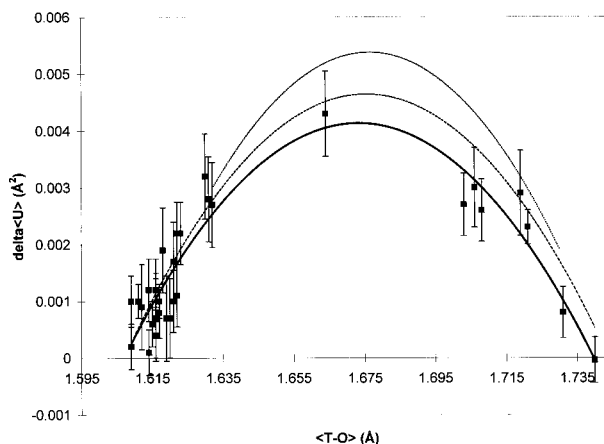


FIGURE 2. Variation of $\langle\Delta U\rangle$ (Å²) as a function of $\langle T-O\rangle$ (Å) in our albite samples with varying (Si, Al) occupation. The heavy solid curve through the data represents the theoretical curve. The dashed curve results from a quadratic regression. The upper dotted curve shows the quadratic regression reported by Kunz and Armbruster (1990). Error bars represent $2\sigma\langle\Delta U\rangle$.

²For a copy of Figure 3, Document AM-99-016, contact the Business Office of the Mineralogical Society of America (see inside front cover of recent issue) for price information. Deposit items may also be available on the American Mineralogist web site (<http://www.minsocam.org> or current web address).

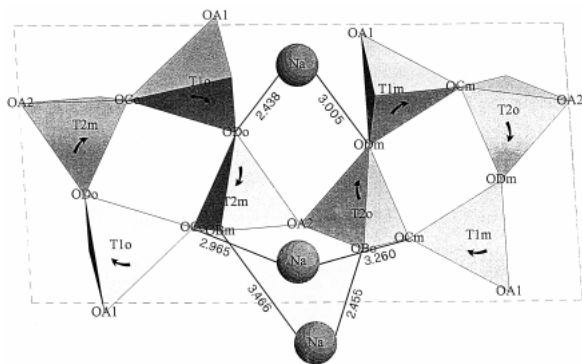


FIGURE 4. Polyhedral projection on the (100) plane of the low albite structure showing the clockwise rotations of the four-membered tetrahedral rings in the (100) plane. Selected Na-O distances as refined for untreated albite are also shown.

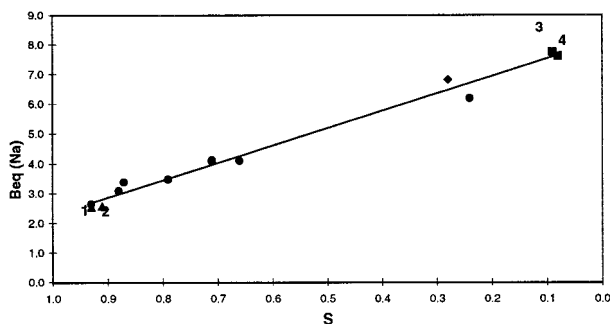


FIGURE 5. Plot of the isotropic equivalent thermal parameter of Na (\AA^2) vs. the order coefficient, S . Circles are for Stintino albites, triangles for low albites (1 = Harlow and Brown 1980; 2 = Armbruster et al. 1990), and squares for high albites (3 = Prewitt et al. 1976; 4 = Winter et al. 1979) measured at room T conditions. The diamond refers to the intermediate albite from Phillips et al. (1989), measured at non ambient conditions. This data has not been included in the regression analysis.

Gottardi 1988). The positional disorder of the oxygen atoms evidently influences the position of sodium too, which varies according to the first neighbors coordinated to it. The increase of $B_{\text{eq}}(\text{Na})$ linearly depends on S (Fig. 5). The regression line is:

$$B_{\text{eq}}(\text{Na}) = 8.01 - 5.73S \quad (6)$$

The $B_{\text{eq}}(\text{Na})$ obtained by Phillips et al. (1989) for an intermediate albite with $S = 0.28$ is equal to 6.82 \AA^2 , greater than the value of 6.18 \AA^2 obtained for our sample 1090-12d, whose degree of disorder is slightly greater ($S = 0.24$). This occurs because the structural refinement of Phillips et al. (1989) was performed at a temperature of 1050 K and pressure of 1.7 GPa. The value of B_{eq} for the disorder found by Phillips et al. (1989) should be around $6.3\text{--}6.4 \text{ \AA}^2$. The difference between this value and the experimental one is probably due to the effective increase in the thermal motion, whereas the difference between the values of B_{eq} for our untreated sample and number 1090-12d can be attributed to the positional disorder of sodium.

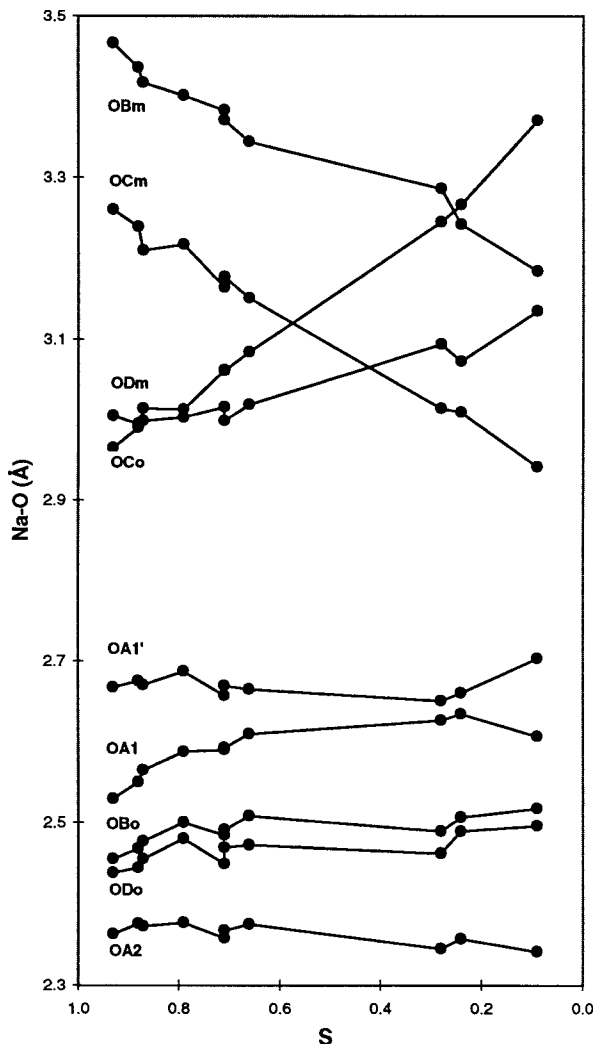


FIGURE 6. Plot of the single Na-O distances vs. the order coefficient S .

Na-O distances as a function of disorder

Some of the Na-O distances (OA2, OBo, ODo) are practically unaffected by the increasing degree of disorder (Fig. 6), whereas others (OBm, OCm, OCo) vary considerably. In particular, Na-OCm is shortened while the Na-OCo is elongated; the average of these two distances, which become equivalent in the monoclinic phase, is always very close to the value which was reported for the Na-OC distance (3.13 \AA) in monalbite (Winter et al. 1979). The same behavior can be recognized, although with a less pronounced variation, for the Na-OBm and Na-OBo couple. In contrast, both the Na-ODm and Na-ODo distances increase; in this case, the average is significantly less than the corresponding distance in monalbite (Na-OD = 2.83 \AA). Such an increase therefore reflects a clear tendency of the average distance to approach the Na-OD distance in monalbite. A likely explanation for the entire process, accounting for geometric constraints and local charge balance requirements, is as follows. The progressive depletion of Al atoms from the T1o sites and their enrichment in the other tet-

rahedral sites causes both a decrease in the T1o polyhedral volume, and an increase of charge on the OCo oxygen. Both these mechanisms are capable of inducing the clockwise shifts of tetrahedral atoms, as shown in Figure 4. The re-distribution of charge on the O atoms, caused by the disordering process, explains the increased regularity of the coordination environment of Na as observed in monalbite. Within this context, one would expect that, when the average distance of each couple (i.e., Na-OCo vs. Na-OCm, etc...) has reached the corresponding value in monalbite, the displacement of the involved atoms would stop. A similar process can be inferred also from the temperature-dependent variations of coordinates in high albite (cf. Fig. 5 in Winter et al. 1979). However, in our case it can be seen that the elongation and shortening of Na-OCo and Na-OCm distances, respectively, goes beyond the crossing point representing their average distance at about $S = 0.6$ (see Fig. 6). It can be observed that the clockwise shift of OCo oxygen causes an out-of-(100) plane tilt of the T2m tetrahedron; this favors a better coordination between OBM and the Na atom located in the adjacent cage. This tilting may well be responsible for the additional elongation of Na-OCo and shortening of Na-OCm observed in our samples with respect to monalbite.

ACKNOWLEDGMENTS

The Ministero della Università e della Ricerca Scientifica e Tecnologica is thanked for the financial support to the research program "Relations between structure and properties in minerals: analysis and applications." C.N.R. of Italy is acknowledged for financial support. The Centro di Strutturistica Diffrattometrica di Ferrara University and CIGS of Modena University are also acknowledged for assistance in the X-ray data collection. The authors thank G. Vezzalini (University of Modena) for chemical analyses and G. Oggiano (University of Sassari) for his help in sample collection.

REFERENCES CITED

- Alberti, A. (1996) The relationship between atomic displacement factors and structural parameters in silica polymorphs. *European Journal of Mineralogy*, 8, 1311–1325.
- Alberti, A. and Gottardi, G. (1985) On the influence of (Si-Al) disorder on the T-O distances measured in zeolites. In B. Drzaj, S. Hocevar, and S. Pejovnik, Eds., *Zeolites Synthesis Structure, Technology and Application*, p. 255–261. Elsevier, Amsterdam.
- (1988) The determination of the Al-content in the tetrahedra of framework silicates. *Zeitschrift für Kristallographie*, 184, 49–61.
- Alberti, A., Gottardi, G., and Lai, T. (1990) The determination of (Si-Al) distribution in zeolites. In D. Barthomeuf, E.G., Derouane, and W. Holderich, Eds., *Guidelines for Mastering the Properties of Molecular Sieves*, p. 145–155. Plenum Press, New York.
- Armbruster, T., Bürgi, H.B., Kunz, M., Gnos, E., Brönnimann, S., and Lienert, C. (1990) Variation of displacement parameters in structure refinements of low albite. *American Mineralogist*, 75, 135–140.
- Blasi, A. and Blasi De Pol, C. (1994) Aspects of alkali feldspar characterization: prospects and relevance to problems outstanding. In I. Parson, Ed., *Feldspars and their reactions*, p. 51–101. Kluwer Academic Publishers, Amsterdam, Netherlands.
- Carpenter, M.A. and Salje, E. (1994) Thermodynamics of nonconvergent cation ordering in minerals: III. Order parameter coupling in potassium feldspar. *American Mineralogist*, 79, 1084–1098.
- Donovan, J.J. (1995) PROBE: PC based data acquisition and processing for electron microprobes. *Advanced Microbeam*, 4217C Kings Graves Road, Vienna, OH, 44473.
- Ferguson, R.B. (1974) A cation-anion distance-dependent method for evaluating valence-bond distributions in ionic structures and results for some olivines and pyroxenes. *Acta Crystallographica*, B30, 2527–2539.
- Griffen, D.T. (1992) *Silicate crystal chemistry*. Oxford University Press, New York.
- Harlow, G.E. and Brown, G.E. (1980) Low albite: an X-ray and neutron diffraction study. *American Mineralogist*, 65, 986–995.
- Hill, R.J. and Gibbs, G.V. (1979) Variation in d(T-O), d(T...T) and -TOT in silica and silicate minerals, phosphates and aluminates. *Acta Crystallographica*, B35, 25–30.
- Jones, J.B. (1968) Al-O and Si-O tetrahedral distances in aluminosilicate framework structures. *Acta Crystallographica*, B24, 355–358.
- Kroll, H. and Ribbe, P.H. (1983) Lattice parameters, composition and Al,Si order in alkali feldspars. (2nd ed.) In *Mineralogical Society of America Short Course Notes*, 2, 57–99.
- Kunz, M. and Armbruster, T. (1990) Difference displacement parameters in alkali feldspars: effects of (Si-Al) order-disorder. *American Mineralogist*, 75, 141–149.
- Phillips, M.W., Ribbe, P.H., and Pinkerton, A.A. (1989) Structure of intermediate albite, NaAlSi₃O₈. *Acta Crystallographica*, C45, 542–545.
- Prewitt, C.T., Sueno, S., and Papike, J.J. (1976) The crystal structures of high albite and monalbite at high temperatures. *American Mineralogist*, 61, 1213–1225.
- Ribbe, P.H. (1975) The chemistry, structure, and nomenclature of feldspars. (1st ed.) In *Mineralogical Society of America Short Course Notes*, 2, 1–72.
- (1983) Chemistry, structure and nomenclature of feldspars. (2nd ed.) In *Mineralogical Society of America Short Course Notes*, 2, 1–19.
- (1984) Average structures of alkali and plagioclase feldspars: systematics and applications. In W.L. Brown, Ed., *Feldspars and feldspathoids: structures, properties and occurrences*, p.1–54. Kluwer Academic Publishers, Amsterdam, The Netherlands.
- (1994) The crystal structures of the aluminum-silicate feldspars. In I. Parson, Ed., *Feldspars and their reactions*, p. 1–49. Kluwer Academic Publishers, Amsterdam, The Netherlands.
- Ribbe, P.H. and Gibbs, G.V. (1969) Statistical analysis and discussion of mean Al/Si-O bond distances and the aluminum content of tetrahedra in feldspars. *American Mineralogist*, 54, 85–94.
- Salje, E. (1985) Thermodynamics of sodium feldspar I: order parameter treatment and strain induced coupling effects. *Physics and Chemistry of Minerals*, 12, 93–98.
- (1988) Kinetic rate laws as derived from order parameter theory I: theoretical concepts. *Physics and Chemistry of Minerals*, 15, 336–348.
- Sheldrick, G.M. (1976) SHELX-76. Program for crystal structure determination. University of Cambridge, Cambridge, UK.
- Smith, J.V. (1954) A review of the Al-O and Si-O distances. *Acta Crystallographica*, 7, 479–483.
- (1974) *Feldspar Minerals*, Vol. 1., 627 p. Springer-Verlag, Berlin.
- Smith, J.V. and Bailey, S.W. (1963) Second review of Al-O and Si-O tetrahedral distances. *Acta Crystallographica*, 16, 801–810.
- Smith, J.V. and Brown, W.L. (1988) *Feldspar Minerals*, Vol. 1. 828 p., Springer-Verlag, Berlin.
- Walker, N. and Stuart, D. (1983) An empirical method for correcting diffractometer data for absorption effects. *Acta Crystallographica*, A39, 158–166.
- Wenk, H.R. and Kroll, H. (1984) Analysis of P1, I1, and C1 plagioclase structures. *Bulletin de Mineralogie*, 107, 467–487.
- Winter, J.K., Okamura, F.P., and Ghose, S. (1979) A high-temperature structural study of high albite, monalbite, and the analbite-monalbite phase transition. *American Mineralogist*, 64, 409–423.
- Wruck, B., Salje, E., and Graeme-Barber, A. (1991) Kinetic rate laws derived from order parameter theory IV: kinetics of Al, Si disordering in sodium feldspars. *Physics and chemistry of minerals*, 17, 700–710.

MANUSCRIPT RECEIVED DECEMBER 23, 1997

MANUSCRIPT ACCEPTED JANUARY 28, 1999

PAPER HANDLED BY RONALD C. PETERSON